OPEN

Molecular Psychiatry (2018) 23, 271–281

www.nature.com/mp

ORIGINAL ARTICLE

Inhibition of $STEP_{61}$ ameliorates deficits in mouse and hiPSC-based schizophrenia models

J Xu[1], BJ Hartley[2,3,14], P Kurup[1,14], A Phillips[4], A Topol[2,3], M Xu[5], C Ononenyi[1], E Foscue[1], S-M Ho[3,6], TD Baguley[7], N Carty[1], CS Barros[8,9], U Müller[8], S Gupta[10], P Gochman[11], J Rapoport[11], JA Ellman[7], C Pittenger[5], B Aronow[10], AC Nairn[5], MW Nestor[4], PJ Lombroso[1,5,12] and KJ Brennand[2,3,13]

The brain-specific tyrosine phosphatase, STEP (STriatal-Enriched protein tyrosine Phosphatase) is an important regulator of synaptic function. STEP normally opposes synaptic strengthening by increasing *N*-methyl D-aspartate glutamate receptor (NMDAR) internalization through dephosphorylation of GluN2B and inactivation of the kinases extracellular signal–regulated kinase 1/2 and Fyn. Here we show that $STEP_{61}$ is elevated in the cortex in the $Nrg1^{+/-}$ knockout mouse model of schizophrenia (SZ). Genetic reduction or pharmacological inhibition of STEP prevents the loss of NMDARs from synaptic membranes and reverses behavioral deficits in $Nrg1^{+/-}$ mice. $STEP_{61}$ protein is also increased in cortical lysates from the central nervous system-specific ErbB2/4 mouse model of SZ, as well as in human induced pluripotent stem cell (hiPSC)-derived forebrain neurons and *Ngn2*-induced excitatory neurons, from two independent SZ patient cohorts. In these selected SZ models, increased $STEP_{61}$ protein levels likely reflect reduced ubiquitination and degradation. These convergent findings from mouse and hiPSC SZ models provide evidence for $STEP_{61}$ dysfunction in SZ.

Molecular Psychiatry (2018) **23,** 271–281; doi:10.1038/mp.2016.163; published online 18 October 2016

INTRODUCTION

$STEP_{61}$, a membrane-associated phosphatase found in the postsynaptic density[1] and endoplasmic reticulum,[2] is highly expressed in the frontal cortex and other forebrain (FB) regions.[3] $STEP_{61}$ activity and degradation are tightly regulated through mechanisms that include inhibitory phosphorylation by protein kinase A at a serine (ser221) within its substrate-binding region (kinase interacting domain)[4] and degradation by the ubiquitin proteasome system (UPS).[5] $STEP_{61}$ is the only STEP (STriatal-Enriched protein tyrosine Phosphatase) isoform detected in the cortex and is elevated in several neuropsychiatric disorders, including fragile X syndrome,[6] Parkinson's disease[7] and Alzheimer's disease[5] (reviewed in Goebel-Goody *et al.*[8] and Karasawa and Lombroso[9]). The mechanisms for increased $STEP_{61}$ include increased translation (fragile X syndrome), disrupted ubiquitination (Parkinson's disease) and beta-amyloid-mediated inhibition of the proteasome (Alzheimer's disease). Amelioration of the biochemical, cognitive and behavioral deficits through either genetic reduction or pharmacological inhibition of STEP activity in mouse models support a relationship between elevated $STEP_{61}$ activity and these disorders.[8,10,11]

We previously reported that $STEP_{61}$ is elevated in postmortem anterior cingulate cortex and dorsolateral prefrontal cortex of schizophrenia (SZ) patients, as well as in mice treated with the psychotomimetics (and *N*-methyl D-aspartate glutamate receptor (NMDAR) antagonists) MK-801 and phencyclidine (PCP).[12] Moreover, the acute (locomotor) and chronic (cognitive) effects of these psychotomimetics were blunted in STEP knockout (KO) mice.[12]

Here we investigated the extent and effect of $STEP_{61}$ dysregulation in two genetic mouse models of SZ ($Nrg1^{+/-}$ and central nervous system (CNS)-specific ErbB2/4 KO mice[13,14]), as well as in two independent cohorts of SZ human induced pluripotent stem cell (hiPSC)-derived neurons. We not only observed increased $STEP_{61}$ activity in both genetic mouse models of SZ and the two cohorts of SZ hiPSC neurons but also that STEP inhibition was sufficient to ameliorate biochemical and behavioral deficits identified in these models. These results suggest an important contribution of $STEP_{61}$ to SZ pathophysiology and thus identify it as a plausible therapeutic target.

MATERIALS AND METHODS

Human induced pluripotent stem cells

SZ1: All SZ1 fibroblasts were obtained from Coriell Institute (Camden, NJ, USA) (P1 (GM02038, male), P2 (GM01792, male), P3 (GM01835, female), P4 (GM02497, male)). Control fibroblasts were obtained from ATCC (Manassas, VA, USA) (C1 (CRL-2522, male)) and Coriell Institute (C2 (GM03440, male), C3 (GM03651, female), C4 (GM04506, female), C5 (AG09319, female), C6 (AG09429, female)). SZ2: The Rapoport laboratory at NIH (Bethesda, MD, USA) generously provided SZ2 fibroblasts from nine cases with childhood-

[1]Child Study Center, Yale University, New Haven, CT, USA; [2]Department of Psychiatry, Icahn School of Medicine at Mount Sinai, New York, NY, USA; [3]Friedman Brain Institute, Icahn School of Medicine at Mount Sinai, New York, NY, USA; [4]Hussman Institute for Autism, Baltimore, MD, USA; [5]Department of Psychiatry, Yale University, New Haven, CT, USA; [6]Department of Developmental and Stem Cell Biology, Icahn School of Medicine at Mount Sinai, New York, NY, USA; [7]Department of Chemistry, Yale University, New Haven, CT, USA; [8]Dorris Neuroscience Center, Department of Cell Biology, The Scripps Research Institute, La Jolla, CA, USA; [9]Plymouth University School of Medicine, Plymouth UK; [10]UC Department of Pediatrics, Cincinnati Children's Hospital Medical Center, Cincinnati, OH, USA; [11]Childhood Psychiatry Branch, National Institute of Mental Health, National Institutes of Health, Bethesda, MD, USA; [12]Department of Neurobiology, Yale University, New Haven, CT, USA and [13]Department of Neuroscience, Icahn School of Medicine at Mount Sinai, New York, NY, USA. Correspondence: Dr PJ Lombroso, Department of Psychiatry, Yale University, New Haven, CT, USA or Dr KJ Brennand, Department of Psychiatry, Icahn School of Medicine at Mount Sinai, 1425 Madison Avenue, New York, NY, 10029, USA.
E-mail: paul.lombroso@yale.edu or kristen.brennand@mssm.edu
[14]These authors contributed equally to this work.
Received 25 February 2015; revised 13 July 2016; accepted 11 August 2016; published online 18 October 2016

onset-SZ and eight controls (C1 (NSB553, male), C2 (NSB690, male), C3 (NSB2607, male), C4 (NSB3084, male), C5 (NSB3158, female), C6 (NSB3182, female), C7 (NSB3234, male), C8 (NSB3113, female), P1 (NSB499, female), P2 (NSB581, male), P3 (NSB676, female), P4 (NSB1442, male), P5 (NSB2513, male), P6 (NSB2620, male), P7 (NSB2011, female), P8 (NSB2476, female), P9 (NSB2962, male)). Copy number variant analysis (SZ1[15]; SZ2[16]) indicates that there is no evidence for any large deletion of NRG1 (or related genes) in either cohort. Detailed description of patients and demographic summary can be found in Supplementary Methods and Supplementary Tables S1 and S2.

SZ1: human fibroblasts were reprogrammed using doxycycline-inducible lentiviral vectors.[15] SZ2: human fibroblasts were reprogrammed using Cytotune Sendai virus (Life Technologies, Carlsbad, CA, USA). All hiPSC lines were validated by: long-term expansion beyond 10 passages; fluorescence-activated cell sorting analysis for SSEA-4 and TRA-1-60 levels; transcript analysis for *OCT4*, *NANOG*, *c-MYC* and *LIN28*; and G-banding analysis to confirm normal karyotypes (Supplementary Figures S5a–c). Detailed description can be found in Supplementary Methods.

hiPSC FB neural progenitor cells (NPCs) were derived, expanded and differentiated using the established methods (SZ1: as described;[15,17] SZ2: as described[18,19] (detailed description can be found in Supplementary Methods and validation in Supplementary Figure S5d)). For *Ngn2*-induced neuronal differentiation, NPCs were transduced with lentiviral TetO-mNgn2-T2A-PuroR (Addgene, Cambridge, MA, USA; ID: 52047) together with a lentiviral constitutive reverse tetracycline transactivator (Addgene ID: 19780); transgene expression was induced with doxycycline (1 μg ml^{-1}; Sigma, St. Louis, MO, USA) for 7 days and selected with puromycin (1 μg ml^{-1}; Sigma) for 24 h. Detailed description can be found in Supplementary Methods.

Rat cortical neurons

All experimental procedures were approved by the Yale University Institutional Animal Care and Use Committee and in strict accordance with the NIH Guide for the Care and Use of Laboratory Animals. Primary cortical neurons were isolated from rat E18 embryos as described.[11,20]

Mice

$Nrg1^{+/-}$ mice were initially obtained from Mutant Mouse Regional Resource Centers supported by NIH (MMRRC Stock Number: 011745-UCD). $Nrg1^{+/-}$ mice were backcrossed with C57BL/6 mice (Jackson Laboratory, Bar Harbor, ME, USA). All mice were genotyped using PCR according to the vendor's protocol. Brains from male $Nrg1^{+/-}$ mice and littermates were collected at several time points (1, 3, 6, 9 and 12 months). All mice were maintained at a controlled temperature and 12 h light/dark cycle with regular diet. Brain lysates from ErbB2/4 CNS KO mice (9 months) were prepared as described[14] and were kindly provided by Dr Müller (Scripps Research Institute, La Jolla, CA, USA).

For biochemical testing, one group of $Nrg1^{+/-}$ mice (male, 6–9 months) and wild-type (WT) littermates were administered intraperitoneally (i.p.) with vehicle (Veh, 0.1% dimethyl sulfoxide in saline), clozapine (Clz, 1 mg kg^{-1}) or haloperidol (Hal, 2 mg kg^{-1}) daily for 2 weeks. A second group of $Nrg1^{+/-}$ and WT mice were administered acutely with Veh (0.1% dimethyl sulfoxide in saline) or TC-2153 (10 mg kg^{-1}) and killed 3 h after injections. Frontal cortices were collected for biochemical analyses.

Genetic and pharmacological testing was carried out in distinct experiments; independent measurements are most appropriately compared within, rather than between, these experiments. For genetic reduction of STEP, $Nrg1^{+/-}$ mice were crossed with $STEP^{-/-}$ mice (on C57BL/6 background as described[12,21] to produce $Nrg1^{+/-}$ mice null for STEP (double mutant); four cohorts were tested (6–9 months old, $n = 9$–16 each group). For pharmacological reduction of STEP, mouse behavioral and cognitive assays were conducted on four cohorts of male $Nrg1^{+/-}$ and WT littermates (6–9 months old, $n = 9$–16 each group). Detailed methodology can be found in Supplementary Methods.

Reagents and antibodies

Reagents are detailed in Supplementary Methods. Antibodies are listed in Supplementary Table S4. Primers are listed in Supplementary Table S5.

Data analysis

For western blotting, phosphorylated protein levels were normalized to total protein levels, then to β-actin as loading control, with one exception: when pGluN2B was evaluated in synaptosomal fractions (P2), pGluN2B levels were normalized to β-actin directly. All data are expressed as means ± s.e.m. and statistical analyses were performed using SPSS Statistics 19 (IBM, New York, NY, USA), Prism 6.0 (GraphPad Software, La Jolla, CA, USA) or JMP10 (SAS Institute, Cary, NC, USA). Significance ($P < 0.05$) was determined by one- or two-way analysis of variance (ANOVA) with *post-hoc* Bonferroni's test (see Figure Legends). For locomotion, data were analyzed with two-way ANOVA with repeated measures, with *post-hoc* Bonferroni's or paired *t*-test. A chi-square one-sample *t*-test against 50% chance was used for social dominance tube test. For both SZ1 hiPSC studies (1–2 independent NPC lines were used per hiPSC, 1 hiPSC per individual (see Supplementary Table S1)) and SZ2 hiPSC experiments (1 NPC line per hiPSC, 1 hiPSC per individual (see Supplementary Table S2)); error bars represent variation (s.e.) between parallel differentiations from the same NPC line.

RESULTS

$STEP_{61}$ is elevated in $Nrg1^{+/-}$, CNS-specific ErbB2/4 KO mice and hiPSC neurons from SZ patients

NRG1[13,22,23] and *ERBB4*[24] have been linked to SZ (reviewed in Mei *et al.*[25]); either reduction or overexpression of Nrg1 signaling results in behavioral and cognitive deficits in animal models.[13,26–28] To investigate the functional implications of $STEP_{61}$ dysregulation in SZ, we analyzed $STEP_{61}$ protein levels in $Nrg1^{+/-}$ and CNS-specific ErbB2/4 KO mice.[13,14] Total $STEP_{61}$ was increased, whereas the phosphorylated (inactive) form of $STEP_{61}$ was decreased in synaptosomal fractions (P2) from frontal cortex of $Nrg1^{+/-}$ mice (Figure 1a). Phosphorylation of the $STEP_{61}$ substrates GluN2B and extracellular signal–regulated kinase 1/2 (ERK1/2), as well as synaptic levels of GluN2B, were decreased in P2 fractions (Figure 1a) in the presence of increased $STEP_{61}$. Analysis of the ratio of synaptic GluN2B versus total GluN2B also revealed a decrease in functional receptors in synaptic membranes (Figure 1a). There was a developmental increase in $STEP_{61}$ levels in $Nrg1^{+/-}$ mice starting at 3 months of age (Supplementary Figure S1a). A similar significant increase in $STEP_{61}$ was observed in ErbB2/4 CNS-specific KO mice, another putative SZ model, with a decrease in the Tyr phosphorylation of GluN2B and ERK1/2 (Supplementary Figure S1b).

We next examined a cohort of six controls and four SZ patients (herein referred to as cohort SZ1: available clinical information is described in Supplementary Table S1, originally described in Brennand *et al.*[15,17]), from which we had previously reprogrammed hiPSCs, differentiated hiPSC neurons and reported synaptic deficits.[15,29] Gene expression comparisons of our hiPSC FB neuron populations to the Allen BrainSpan Atlas indicate that these cells, from both controls and SZ patients, resemble fetal rather than adult brain tissue, particularly the cortical and subcortical FB regions.[17] FB neuron populations are comprised of ~80% neurons and ~20% astrocytes;[15] moreover, the majority of FB neurons are VGLUT1-positive and so are presumably glutamatergic, although approximately 30% are GAD67-positive (GABAergic) and a small minority are TH-positive (dopaminergic).[15,17]

Perturbations in the GluN2A/GluN2B subunit ratio (encoded by the *GRIN2A* and *GRIN2B* genes) are thought to reflect synaptic deficits.[30] Over the course of hiPSC FB neuronal differentiation, *GluN2A* expression increases with no change in *GluN2B*, resulting in an increased *GluN2A/GluN2B* mRNA ratio (Supplementary Figure S2a). SZ1-FB neurons had a decreased *GluN2A/GluN2* mRNA ratio (decreased expression of *GluN2A* while *GluN2B* was unchanged[15,17,31]) (Supplementary Figure S2b) and a decreased GluN2A/GluN2B protein ratio (decreased GluN2A protein in SZ1-FB neurons with no significant change in GluN2B protein levels) (Supplementary Figures S2c – e).

We observed a significant increase of total $STEP_{61}$ ($tSTEP_{61}$) and active, non-phosphorylated $STEP_{61}$ ($aSTEP_{61}$) in SZ1-FB hiPSC neurons. Data are presented both by group average (Figure 1b) and by individuals (Supplementary Figure S3). Increased $STEP_{61}$

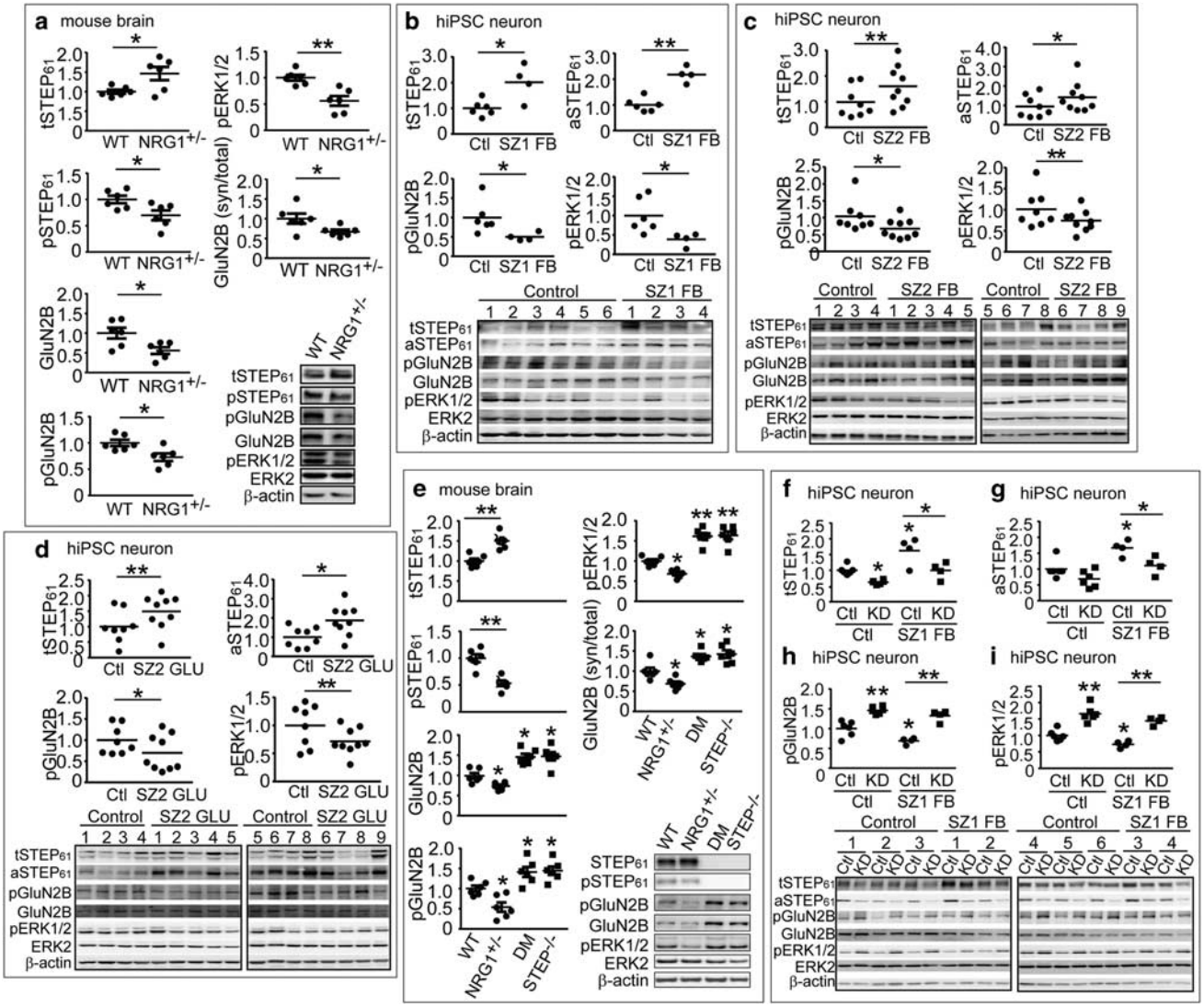

Figure 1. $STEP_{61}$ level is elevated in $Nrg1^{+/-}$ mice and human induced pluripotent stem cell (hiPSC) neurons from schizophrenia (SZ) patients. (**a**) $STEP_{61}$ level is elevated in $Nrg1^{+/-}$ mice. P2 membrane fractions from 9-month-old $Nrg1^{+/-}$ mice were processed by western blotting (WB) using antibodies against total $STEP_{61}$, phosphorylated $STEP_{61}$ (p$STEP_{61}$, inactive) and tyrosine phosphorylation of STEP substrates GluN2B and ERK1/2. All antibodies are listed in Supplementary Table S4. (**b**–**d**) $STEP_{61}$ level is elevated in SZ hiPSC neurons. Total $STEP_{61}$ (t$STEP_{61}$), active $STEP_{61}$ (a$STEP_{61}$) and Tyr phosphorylation of STEP substrates (GluN2B and ERK1/2) levels were probed in SZ1 forebrain (FB) neurons (**b**), SZ2-FB hiPSC neurons (**c**) and SZ2 *Ngn2*-induced excitatory (GLU) neurons (**d**). Detailed description of patients and demographic summary can be found in Supplementary Methods and Supplementary Tables S1 and S2 (**e**) Tyr phosphorylation of STEP substrates is restored in $Nrg1^{+/-}$ mice null for STEP. P2 fractions from wild-type (WT), $Nrg1^{+/-}$, $STEP^{-/-}$ and $Nrg1^{+/-}$ $STEP^{-/-}$ (double mutant, DM) mice were processed by WB and probed for targets shown in the figure. (**f**–**i**) STEP lentiviral (LV) short hairpin RNA knockdown (KD), relative to LV-scrambled control (Ctl), resulted in significantly decreased t$STEP_{61}$ (**f**) and a$STEP_{61}$ (**g**) levels and increased phosphorylation of the $STEP_{61}$ substrates pGluN2B (**h**) and pERK1/2 (**i**) in SZ1-FB hiPSC neurons. Mice data are expressed as mean ± s.e.m. and statistical significance was determined using one-way analysis of variance (ANOVA) with Bonferroni's test (*$P < 0.05$, **$P < 0.01$, $n = 6$ each group). hiPSC neuron data are expressed as mean values from 3 to 6 replicates and statistical significance was determined by nested ANOVA analyses (*$P < 0.05$, **$P < 0.01$, SZ1-FB: 6 controls and 4 patients; SZ2-FB and SZ2-GLU: 8 controls and 9 patients).

was associated with decreased phosphorylation of GluN2B (Figure 1b; Supplementary Figure S3c) and ERK1/2 (Figure 1b; Supplementary Figure S3d) at the sites dephosphorylated by STEP. We also measured $STEP_{61}$ levels in SZ1 fibroblasts, hiPSCs and in replicating NPCs. $STEP_{61}$ protein was not detected in fibroblast cultures and, although present, showed no increase in SZ1 hiPSCs (Supplementary Figures S4a and b) or NPCs (Supplementary Figures S4c and d). These results indicate that the increase in $STEP_{61}$ is only detectable in postmitotic SZ1-FB hiPSC neurons.

To validate these findings, we established a second cohort of SZ hiPSCs, comprising eight controls and nine SZ patients (herein referred to as SZ2: available clinical information is described in Supplementary Table S2; fluorescence-activated cell sorting validation for all hiPSCs (TRA-1-60 and SSEA4) and NPCs (NESTIN and SOX2) is shown in Supplementary Figure S5; partially reported in Topol *et al.*[19]). Consistent with our observations from SZ1, SZ2-FB hiPSC neurons showed increased total $STEP_{61}$ (Figure 1c; Supplementary Figure S6a) and active $STEP_{61}$ (Figure 1c; Supplementary Figure S6b), which correlated with decreased phosphorylation of GluN2B (Figure 1c; Supplementary Figure S6c) and ERK1/2 (Figure 1c; Supplementary Figure S6d). Moreover, because SZ2 hiPSCs were not generated using

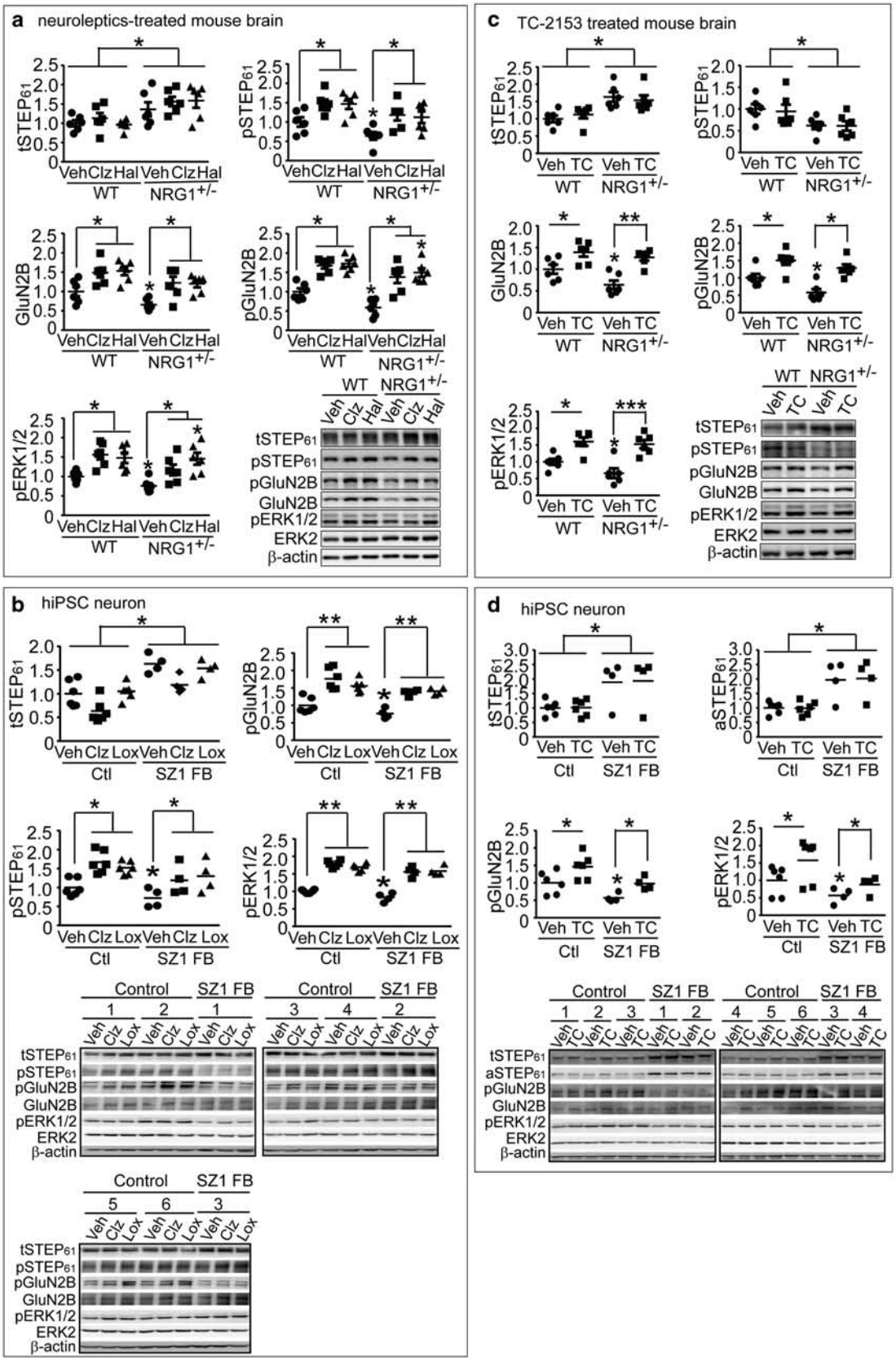
a neuroleptics-treated mouse brain
tSTEP61
pSTEP61
GluN2B
pGluN2B
pERK1/2
Veh Clz Hal Veh Clz Hal
WT NRG1+/-
WT NRG1+/-
Veh Clz Hal
tSTEP61
pSTEP61
pGluN2B
GluN2B
pERK1/2
ERK2
β-actin
c TC-2153 treated mouse brain
Veh TC Veh TC
WT NRG1+/-
WT NRG1+/-
Veh TC
tSTEP61
pSTEP61
pGluN2B
GluN2B
pERK1/2
ERK2
β-actin
b hiPSC neuron
Veh Clz Lox Veh Clz Lox
Ctl SZ1 FB
Control SZ1 FB
1 2 1
3 4 2
5 6 3
Veh Clz Lox
tSTEP61
pSTEP61
pGluN2B
GluN2B
pERK1/2
ERK2
β-actin
d hiPSC neuron
Veh TC Veh TC
Ctl SZ1 FB
tSTEP61
aSTEP61
pGluN2B
GluN2B
pERK1/2
ERK2
β-actin
Control SZ1 FB
1 2 3 1 2
4 5 6 3 4
Veh TC

tetracycline-inducible methods, we were also able to apply a well-established *Ngn2*-induction method to yield populations of nearly pure excitatory (SZ2-GLU) neurons (Supplementary Figure S7);[32,33] critically, these *Ngn2*-induced GLU populations show no evidence for including GABAergic or dopaminergic neurons.[32,33] SZ2-GLU hiPSC neurons showed increased total (Figure 1d; Supplementary Figure S8a) and active (Figure 1d; Supplementary Figure S8b) $STEP_{61}$ levels, which again correlated with decreased phosphorylation of GluN2B (Figure 1d; Supplementary Figure S8c) and ERK1/2 (Figure 1d; Supplementary Figure S8d), indicating that increased $STEP_{61}$ could be specifically detected in defined populations of excitatory neurons derived from SZ2 patients. Increased $STEP_{61}$ levels were driven by a subset of patients (a one-sample two-tailed *t*-test found that three of the four of SZ1-FB, four of the nine of SZ2-FB and three of the nine of SZ2-GLU neuron samples tested showed evidence of elevated $STEP_{61}$ levels) (Supplementary Table S3). Increased STEP activity in SZ2 GLU neurons in no way excludes the possibility that STEP levels are also perturbed in other neuronal or glial cell populations.

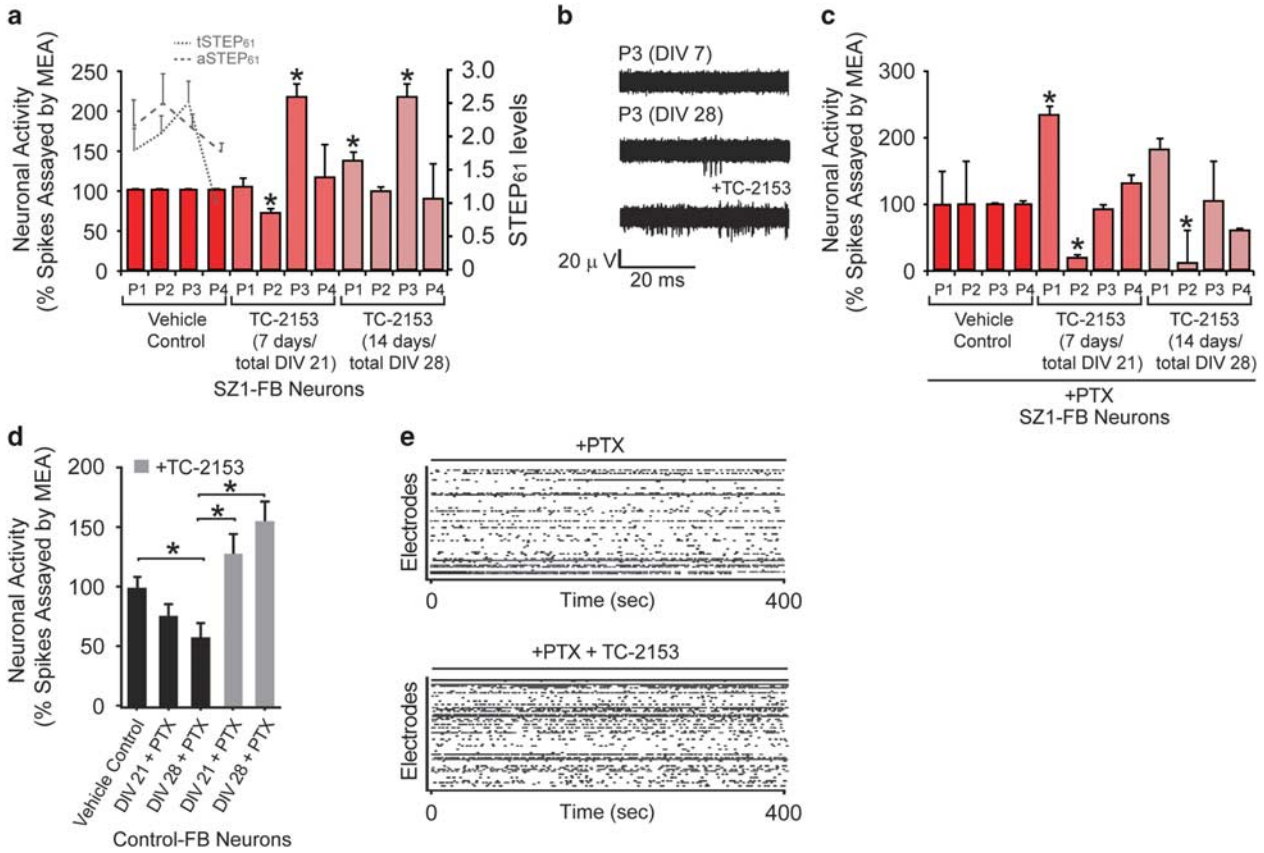

Figure 3. STEP inhibitor increases spontaneous neuronal activity in human induced pluripotent stem cell (hiPSC) neurons. (**a**) Multi-electrode array (MEA) analysis reveals that treatment with TC-2153 (1 μM), for either the final 7 or 14 days of differentiation, increased the rate of spontaneous neuronal firing in SZ1-FB hiPSC neurons from two patients with most elevated $STEP_{61}$ levels. Dotted (total $STEP_{61}$) and dashed (active $STEP_{61}$) lines indicate relative basal $STEP_{61}$ protein levels in SZ1-FB hiPSC neurons from each SZ patient. (**b**) Representative raw MEA cumulative neuronal spike activity showing the effect of TC-2153 (1 μM) on SZ1-FB hiPSC neurons. (**c**) Acute pharmacological inhibition of SZ1-FB hiPSC neurons with picrotoxin (PTX) (30 min, 50 μM), when combined with MEA analysis, reveals that chronic TC-2153 (1 μM) treatment (7 or 14 days) affects firing of excitatory neurons. (**d**) MEA analysis of one control hiPSC line showing that acute PTX (50 μM) treatment for 30 min results in decreased neuronal spiking, but when combined with chronic TC-2153 treatment (7 or 14 days), neuronal activity is increased compared with PTX treatment alone. (**e**) Representative raw MEA traces of neuronal activity showing the effect of TC-2153 (1 μM), in the presence of PTX (50 μM), on control hiPSC neurons. For all experiments, in each condition, six replicates per neural progenitor cell line were tested (*$P < 0.05$, one-way analysis of variance with Fisher's *post-hoc*, SZ1-FB: 1 control and 4 patients). SZ, schizophrenia.

Figure 2. Pharmacological inhibition of $STEP_{61}$ restores *N*-methyl D-aspartate glutamate receptor biochemical signaling in $Nrg1^{+/-}$ mice and human induced pluripotent stem cell (hiPSC) neurons. (**a**) Antipsychotic administration leads to inactivation of $STEP_{61}$ and increases in Tyr phosphorylation of GluN2B and ERK1/2 *in vivo*. Wild-type (WT) and $Nrg1^{+/-}$ mice were administered clozapine (Clz, 1 mg kg^{-1}, intraperitoneally (i.p.)), haloperidol (Hal, 2 mg kg^{-1}, i.p.) or vehicle (Veh) daily for 2 weeks. Changes in phosphorylation of $STEP_{61}$ and its substrates in P2 fractions were analyzed by western blotting (WB). (**b**) Antipsychotics Clz (5 μM) and loxapine (Lox 10 μM) resulted in phosphorylation and inactivation of $STEP_{61}$ and subsequent increases in Tyr phosphorylation of GluN2B and ERK1/2 in control and SZ1-FB hiPSC neurons. (**c**) WT and $Nrg1^{+/-}$ mice were administered TC-2153 (TC, 10 mg kg^{-1}, i.p.) or vehicle (Veh) acutely for 3 h. P2 fractions were used to probe for STEP and its substrates by WB. Mice data are expressed as mean ± s.e.m. and statistical significance was determined using one-way analysis of variance with Bonferroni's test (*$P < 0.05$, **$P < 0.01$, ***$P < 0.001$, $n = 6$ each group). (**d**) TC-2153 treatment leads to significantly increased pGluN2B and pERK1/2 levels in control and SZ1-FB hiPSC neurons, without altering $tSTEP_{61}$ or $aSTEP_{61}$ levels. hiPSC neuron data are expressed as mean values from 3 to 6 replicates and statistical significance was determined by nested ANOVA analyses using JMP statistical software (*$P < 0.05$, **$P < 0.01$, SZ1-FB: 6 controls and 4 patients).

Genetic reduction of $STEP_{61}$ increases phosphorylation of STEP targets in $Nrg1^{+/-}$ mice and hiPSC neurons

$Nrg1^{+/-}$ mice null for $STEP_{61}$ (double mutant (DM)) showed restored tyrosine phosphorylation levels of GluN2B and ERK1/2 (Figure 1e).[21,34] Genetic reduction of *STEP* in $Nrg1^{+/-}$ mice also rescued functional GluN2B-containing receptors at synaptic sites, as measured by synaptic versus total receptor levels (Figure 1e). Similarly, $STEP_{61}$ knockdown in hiPSC neurons using lentiviral

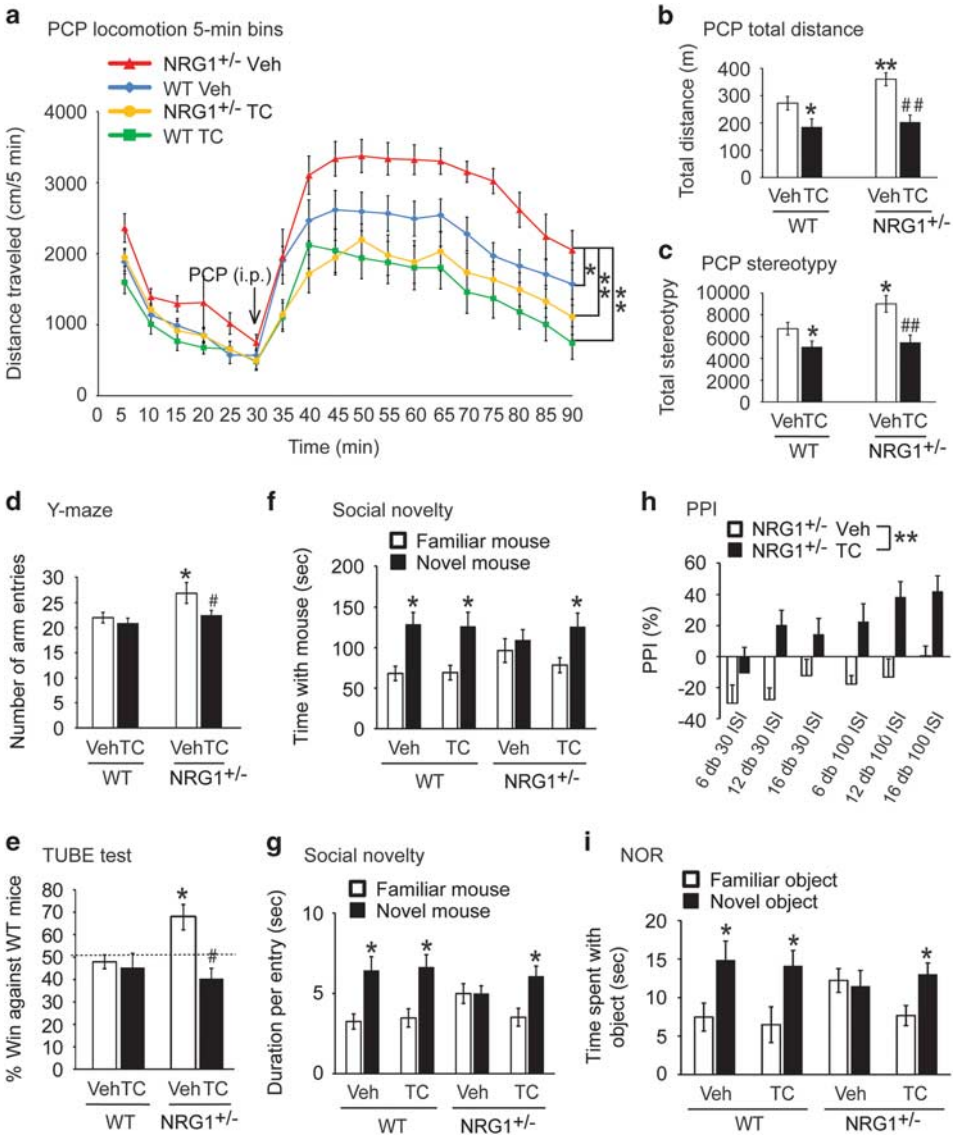

Figure 4. STEP inhibition reverses behavioral and cognitive deficits in $Nrg1^{+/-}$ mice. Male wild-type (WT) and $Nrg1^{+/-}$ littermates (6–9 months old, 9–16 male mice each group) were used for all tests. (**a**–**c**) Pharmacological inhibition of $STEP_{61}$ normalizes phencyclidine (PCP)-induced hyperlocomotor activity and stereotypies. Mice were administered TC-2153 (TC, 10 mg kg^{-1}, intraperitoneally (i.p.)) or vehicle (Veh) and monitored for basal activities for 30 min. Mice were then challenged with PCP (7.5 mg kg^{-1}, i.p.) for 1 h. Distance traveled in each 5 min bin during the 90 min test period (**a**), total distance traveled (**b**) and total stereotypic counts (**c**) were recorded and analyzed using Activity Monitor (MED Associates). (**d**) $Nrg1^{+/-}$ mice made more entries in Y-maze; this was reversed 3 h after TC-2153 treatment. (**e**) TC-2153 administration normalizes aggressive behavior in $Nrg1^{+/-}$ mice. Mice were administered TC-2153 (TC, 10 mg kg^{-1}, i.p.) or Veh. Three hours after injection, mice were tested in a narrow plastic tube against non-littermate naive WT mice. Each mouse went through four trials and percentage of win was plotted. (**f**, **g**) TC-2153 administration improves social behavior in the social novelty task in $Nrg1^{+/-}$ mice. Mice were administered TC-2153 (TC, 10 mg kg^{-1}, i.p.) or Veh. Three hours after injection, mice were tested in three-chamber social task. Behaviors in the first two stages (habituation and social preference) are shown in Supplementary Figure S10. (**h**) TC-2153 treatment reversed prepulse inhibition (PPI) deficits in $Nrg1^{+/-}$ mice. $Nrg1^{+/-}$ mice were treated with TC or Veh 3 h prior to PPI test. (**i**) TC-2153 reverses cognitive deficits in $Nrg1^{+/-}$ mice in the novel object recognition (NOR) task. Mice were administered TC-2153 (TC, 10 mg kg^{-1}, i.p.) or Veh. Three hours after injection, mice were trained with two identical objects. Twenty-four hours after training; mice were tested in the choice phase with one familiar object and one novel object. All data are expressed as mean ± s.e.m. and statistical significance was determined using two-way analysis of variance (ANOVA) with repeated-measures (RM) followed by *post-hoc* Bonferroni's test for panel (**a**) or two-way ANOVA with *post-hoc* Bonferroni's test for panels (**b**–**d**) or RM-ANOVA for panel (**h**) or chi-square one-sample *t*-test against 50% chance for panel (**e**) or Student's *t*-test comparing two objects for panels (**f**, **g**, **i**) (*$P < 0.05$, **$P < 0.01$, compared with the WT Veh group; $^{\#}P < 0.05$, $^{\#\#}P < 0.01$ compared with $Nrg1^{+/-}$ Veh group, $n = 9$–16 per group).

short hairpin RNA reduced total (Figure 1f) and active (Figure 1g) $STEP_{61}$ levels in SZ1-FB hiPSC neurons and increased phosphorylation of pGluN2B (Figure 1h) and pERK1/2 (Figure 1i).

Pharmacological inhibition of STEP increases phosphorylation of STEP targets in $Nrg1^{+/-}$ mice and hiPSC neurons

Several neuroleptics, including Clz, risperidone and Hal, are known to result in inhibitory phosphorylation of $STEP_{61}$ by protein kinase A.[12] To test whether antipsychotic treatment was sufficient to reduce elevated $STEP_{61}$ activity in $Nrg1^{+/-}$ mice, WT mice were administered Veh, Clz (1 mg kg^{-1}, i.p.) or Hal (2 mg kg^{-1}, i.p.) daily for 2 weeks. Indeed, western blotting analysis of P2 fractions demonstrated that, in WT mice, neuroleptic treatment decreased $STEP_{61}$ activity without changing total $STEP_{61}$ levels, leading to an overall increase in the phosphorylation of $STEP_{61}$ substrates (Figure 2a). Similarly, neuroleptic treatment decreased $STEP_{61}$ activity without changing total $STEP_{61}$ levels in $Nrg1^{+/-}$ mice, leading to an overall increase in the phosphorylation of $STEP_{61}$ substrates, often above baseline WT levels (Figure 2a). These observations are in agreement with a previous finding that Clz restores the tyrosine phosphorylation of GluN2B at Tyr^{1472} in $Nrg1^{+/-}$ mice.[35] In both control and SZ1-FB hiPSC neurons, we similarly observed that 7-day treatment with Clz (5 μM) or loxapine (10 μM) decreased $STEP_{61}$ activity and increased the phosphorylation GluN2B and ERK1/2, without affecting total $STEP_{61}$ levels (Figure 2b).

We recently characterized the dose responses, time kinetics and specificity of a novel inhibitor of STEP (8-(trifluoromethyl)-1,2,3,4,5-benzo pentathiepin-6-amine hydro-chloride), known as TC-2153.[11] TC-2153 showed relative specificity for $STEP_{61}$, selectively inhibiting STEP in the cortex and hippocampus, but not two other closely related protein tyrosine phosphatases (PTPs; that is, PTP-SL in the cerebellum and HePTP in the spleen).[11] It also reversed the biochemical and cognitive deficits in a mouse model of Alzheimer's disease,[11] a disorder also characterized by a significant elevation of cortical and hippocampal $STEP_{61}$ levels.[10] TC-2153 treatment of both WT and $Nrg1^{+/-}$ mice produced increased tyrosine phosphorylation of GluN2B and ERK1/2 (Figure 2c). TC-2153 also inhibited $STEP_{61}$ activity in control and SZ1-FB hiPSC neurons, without changing total $STEP_{61}$ levels (Figure 2d). Treatment of control and SZ1-FB hiPSC neurons with 1 μM TC-2153 led to an increase in the Tyr phosphorylation of pGluN2B and pERK1/2 (Figure 2d) that was comparable to Clz or loxapine treatment (Figure 2b).

STEP inhibition increases spontaneous neuronal activity in hiPSC neurons

We tested the effect of chronic 1 μM TC-2153 treatment for 7 or 14 days on spontaneous neuronal activity in control and SZ1-FB hiPSC neurons using multi-electrode array recordings. In two of the three SZ1 patients with elevated $STEP_{61}$ activity (see Supplementary Figure S3 for relative $STEP_{61}$ levels in each patient), 14 days of administration with TC-2153 was sufficient to significantly increase the rate of neuronal firing in cells from these patients (Figures 3a and b). For one of the patients (and one evaluated control), this was also true in the presence of acute (30 min) treatment with 50 μM picrotoxin, a non-competitive channel blocker for the $GABA_A$ receptor, indicating that changes resulting from TC-2153 may reflect changes to the glutamatergic network (Figures 3c–e).

STEP inhibition reverses behavioral and cognitive deficits in $Nrg1^{+/-}$ mice

We tested whether TC-2153 could reverse the behavioral and cognitive deficits in $Nrg1^{+/-}$ mice, which show increased locomotion and disrupted working memory and cognition.[13,28] First, we tested whether TC-2153 was effective in reversing PCP-induced hyperlocomotion in WT and $Nrg1^{+/-}$ mice. Following PCP administration (7.5 mg kg^{-1}, i.p.), a two-way ANOVA with repeated-measures analysis demonstrated significant main effects of Time (5 min bin: $F(17,952) = 52.35$, $P < 0.0001$), Group (4 groups: $F(3,56) = 7.87$, $P < 0.001$) and a Time × Group interaction ($F(51,952) = 1.78$, $P < 0.001$). Bonferroni's *post-hoc* test showed significant attenuation of PCP-induced hyperlocomotion in $Nrg1^{+/-}$ mice by TC-2153 ($P < 0.01$, compared with Veh-treated $Nrg1^{+/-}$ mice) (Figure 4a). Two-way ANOVA analysis of total distance traveled showed that there were significant effects of Treatment (Veh or TC-2153, $F(1,54) = 20.73$, $P < 0.001$) and Genotype (WT or $Nrg1^{+/-}$, $F(1,54) = 4.92$, $P < 0.05$). Bonferroni's *post-hoc* test also revealed that TC-2153 led to a significant attenuation of PCP-induced hyperactivity in $Nrg1^{+/-}$ mice ($P < 0.01$, compared with the Veh/$Nrg1^{+/-}$ group (Figure 4b). In addition, pretreatment of Veh or TC-2153 had a significant effect on stereotypies (such as sniffing, rearing and grooming) ($F(1,55) = 21.67$, $P < 0.001$) and there was a significant main effect of Genotype (WT or $Nrg1^{+/-}$, $F(1,55) = 6.90$, $P < 0.05$). Bonferroni's *post-hoc* test revealed TC-2153 also attenuated PCP-induced stereotypies in $Nrg1^{+/-}$ mice ($P < 0.01$) (Figure 4c). TC-2153 (10 mg kg^{-1}, i.p.) also normalized locomotor activity in the open field (Supplementary Figures S9a and b). Next we tested WT and $Nrg1^{+/-}$ mice in the Y-maze task. We found no difference in arm alternation in these mice (Supplementary Figure S9c). However, we found $Nrg1^{+/-}$ mice made more arm entries, indicating that $Nrg1^{+/-}$ mice were hyperactive in the Y-maze. Administration of TC-2153 reversed hyperactivity in the Y-maze (Figure 4d). Two-way ANOVA analysis of arm entries showed that there were significant effects of Treatment (Veh or TC-2153, $F(1,53) = 7.27$, $P < 0.01$) and Genotype (WT or $Nrg1^{+/-}$, $F(1,53) = 9.35$, $P < 0.01$). Bonferroni's *post-hoc* test showed that TC-2153 reduced arm entries in $Nrg1^{+/-}$ mice ($P < 0.05$, compared with Veh/$Nrg1^{+/-}$ group (Figure 4d). Furthermore, TC-2153 reduced aggression in $Nrg1^{+/-}$ mice (Figure 4e) and significantly improved social behavior in a social novelty task (Figures 4f and g).

Because the motor abnormalities observed in $Nrg1^{+/-}$ mice (Figures 4a–c; Supplementary Figures S9a and b) may confound social behavioral measures, we next conducted a number of non-motor behavioral assays. Mice with deficits in Nrg1 signaling have been reported to show deficits in prepulse inhibition (PPI);[36,37] we also observed deficits in PPI in $Nrg1^{+/-}$ mice (Supplementary Figure S9n). Repeated-measures ANOVA analyses revealed that TC-2153 normalized PPI (Figure 4h) with main effects of Treatment (Veh or TC, $F(1,18) = 11.43$, $P < 0.001$), Interval (30 or 100 ms, $F(1, 18) = 13.71$, $P < 0.001$) and Intensity (+6, +12 or +16 db, $F(2,17) = 3.67$, $P < 0.05$). TC-2153 treatment did not alter PPI in WT mice (Supplementary Figure S9o). There was no difference in startle response in the different treatment groups (Supplementary Figure S9p). TC-2153 also improved the ability of $Nrg1^{+/-}$ mice to distinguish between novel and familiar objects in the novel object recognition task (Figure 4i). Clz (1 mg kg^{-1}, i.p.), which served as a positive control, had similar significant effects in all the tasks (Supplementary Figure S10).

Our previous findings[12,38] suggested that genetic reduction of STEP was sufficient to reduce the biochemical and behavioral changes induced by the NMDAR antagonist PCP. To further demonstrate that pharmacological inhibition of STEP was sufficient to ameliorate the behavioral effects arising from NMDAR antagonism, we used another NMDAR blocker, MK-801, which has been widely validated as a pharmacological model of SZ and induces motor and cognitive deficits in mice.[39–41] In agreement with previous reports,[42,43] we found that MK-801 treatment induced hyperactivity (Supplementary Figures S11a–c) and memory deficits in the Y-maze and novel object recognition tasks (Supplementary Figures S11d and e); these deficits were significantly reversed by pretreatment with TC-2153 (Supplementary Figures S11a–e). Although MK-801 led to reduced GluN2B/GluN1 in synaptosomal membranes (P2) and decreased

phosphorylation of ERK1/2, this was completely rescued by TC-2153 (Supplementary Figure S11f).

We tested whether genetic reduction of $STEP_{61}$ in $Nrg1^{+/-}$ mice would recapitulate the effects of TC-2153. $Nrg1^{+/-}$ mice were hyperactive in the open-field test; this hyperactivity was reduced in DM mice (Supplementary Figures S12a and b). $Nrg1^{+/-}$ hyperactivity after PCP administration was significantly reduced in DM mice (Supplementary Figures S12c–e). In the social

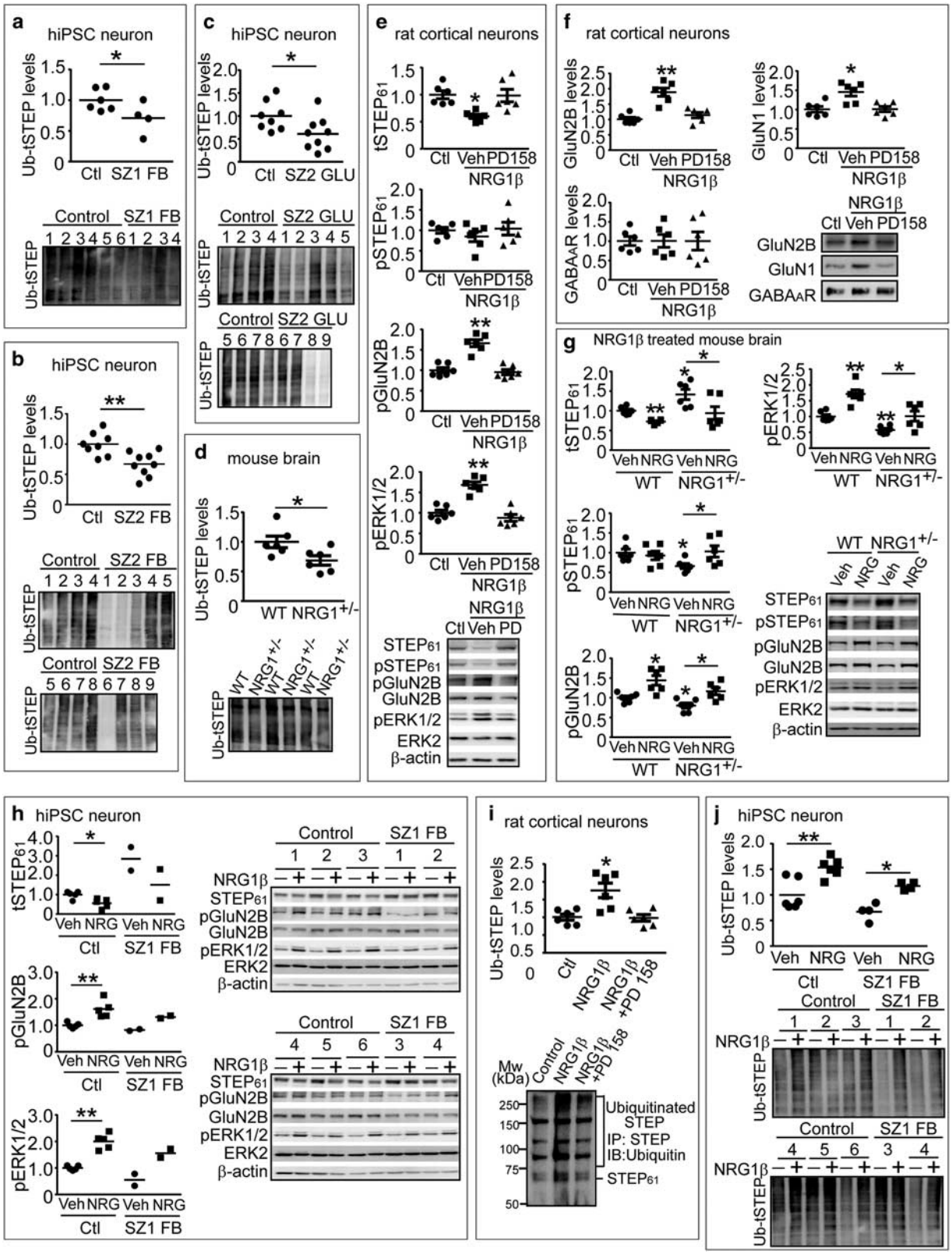

dominance task, aggressiveness in $Nrg1^{+/-}$ mice was normalized in DM mice (Supplementary Figure S12f). In a Y-maze test of working memory, $Nrg1^{+/-}$ mice were normal in terms of alternation choices (Supplementary Figure S10c) but made significantly more arm entries; this was normalized in DM mice (Supplementary Figures S12g and h). In the novel object recognition task, $Nrg1^{+/-}$ mice failed to distinguish between novel and familiar objects, while DM mice behaved similarly to WT mice (Supplementary Figure S12i). Finally, deficient social recognition in $Nrg1^{+/-}$ mice was normalized in DM mice (Supplementary Figure S13). Taken together, these experiments establish that both genetic reduction and pharmacological inhibition of STEP attenuate the biochemical, behavioral and cognitive deficits in $Nrg1^{+/-}$ mice.

NRG1 signaling leads to ubiquitination and degradation of $STEP_{61}$ in rat cortical neurons and hiPSC neurons

$STEP_{61}$ mRNA levels were not different in SZ1-FB hiPSC neurons as measured using quantitative real-time PCR (Supplementary Figure S14a), suggesting that increased transcription of STEP does not contribute to the elevation of $STEP_{61}$ protein levels in these neurons. Likewise, there was no detectable increase in $STEP_{61}$ mRNA in $Nrg1^{+/-}$ mice (Supplementary Figure S14b).

Because $STEP_{61}$ is normally regulated by the UPS, a process that is disrupted in SZ,[12] Parkinson's disease[7] and Alzheimer's disease mouse models,[10,44] we tested the hypothesis that disruption of $STEP_{61}$ ubiquitination contributed to the elevated $STEP_{61}$ levels seen in our SZ models. We observed decreased ubiquitination of total $STEP_{61}$ in SZ1-FB hiPSC neurons (Figure 5a), SZ2-FB hiPSC neurons (Figure 5b) and SZ2-GLU hiPSC neurons (Figure 5c). There was a general decrease of ubiquitinated proteins (Supplementary Figure S15a) and perturbed levels in some (UBE2N, UBA6) UPS proteins in SZ1-FB hiPSC neurons (Supplementary Figures S15c, e, g, i and k). Similarly, we observed decreased ubiquitination of total STEP in frontal cortex from $Nrg1^{+/-}$ mice (Figure 5d). Here, while we did not observe a general decrease of ubiquitinated proteins (Supplementary Figure S15b) or perturbations in most UPS proteins (Supplementary Figures S15d, f, h, j and l), there was again a disruption of UBE2N levels (Supplementary Figure S15d) in $Nrg1^{+/-}$ mice.

We next asked whether NRG1 signaling regulates $STEP_{61}$ levels. NRG1β treatment of WT rat cortical neurons (10 nM, 30 min) led to decreased $STEP_{61}$ levels; this was blocked by PD158780, a pan-ErbB receptor antagonist (Figure 5e). Concomitant with decreased $STEP_{61}$, there was increased tyrosine phosphorylation of GluN2B and ERK1/2 (Figure 5e) and increased surface levels of GluN2B and GluN1, all blocked by PD158780 (Figure 5f). The $GABA_A$ receptor, which is not a $STEP_{61}$ substrate, showed no changes following NRG1β treatment (Figure 5f). The NRG1β extracellular domain (50 ng kg^{-1}, i.p.) crosses the brain–blood barrier and is an effective activator of NRG1 signaling.[45–47] When injected into $Nrg1^{+/-}$ mice (i.p.) daily for 5 consecutive days, NRG1β extracellular domain led to a significant reduction of $STEP_{61}$ and an increase in the tyrosine phosphorylation of the $STEP_{61}$ substrates GluN2B and ERK1/2 (Figure 5g). Similarly, NRG1β treatment of control and SZ1-FB hiPSC neurons resulted in a significant reduction of $STEP_{61}$ and an increase in the tyrosine phosphorylation of GluN2B and ERK1/2 (Figure 5h).

Finally, we examined whether NRG1 signaling can directly affect $STEP_{61}$ ubiquitination. NRG1β treatment (10 nM, 30 min) of WT rat cortical neurons increased ubiquitination (Figure 5i) and proteasome-dependent degradation (Figure 5i) of $STEP_{61}$. Although $STEP_{61}$ can be proteolysed by calpain after excitotoxic conditions,[20] inhibition of calpain, caspase and lysozyme demonstrated that they were not involved in $STEP_{61}$ degradation (Supplementary Figure S16). We repeated these experiments in SZ1-FB hiPSC neurons and assayed the levels of $STEP_{61}$ ubiquitination after NRG1β treatment. Consistent with our observations in rodents, NRG1β treatment increased $STEP_{61}$ ubiquitination and degradation in both control and SZ1-FB hiPSC neurons (Figure 5j).

DISCUSSION

Here we demonstrate that $STEP_{61}$ protein levels are elevated in two mouse models of SZ ($Nrg1^{+/-}$ and CNS-specific ErbB2/4 KOs), as well as two populations of hiPSC-derived (FB and GLU) neurons, from two independent cohorts of SZ patients (similarities and discrepancies between the mouse and human models are summarized in Supplementary Table S6). Genetic or pharmacological reduction of $STEP_{61}$ activity in both mouse and hiPSC-based SZ models increased the phosphorylation of STEP targets, altered neuronal activity and ameliorated cognitive and behavioral deficits. These results reveal a convergence of mouse and hiPSC studies, consistent with our previously reported postmortem data[12] (although see Lanz *et al.*[48]). Elevated $STEP_{61}$ levels were driven by a subset (~50%) of our SZ1 and SZ2 hiPSC neurons; our results must next be replicated across larger cohorts of SZ patients

Figure 5. NRG1 signaling leads to ubiquitination and degradation of $STEP_{61}$ in rat cortical neurons and human induced pluripotent stem cell (hiPSC) neurons. (**a**–**c**) Ubiquitination of STEP is decreased in schizophrenia hiPSC neurons. Ubiquitinated protein were pulled down from SZ1-FB hiPSC neurons (**a**), SZ2-FB hiPSC neurons (**b**) or SZ2-GLU hiPSC neurons (**c**) using tandem ubiquitin binding entities (TUBE) agarose beads as described in Supplementary Methods, followed by detection with anti-STEP antibody. (**d**) Ubiquitination of STEP is decreased in $Nrg1^{+/-}$ mice. Male wild-type (WT) and $Nrg1^{+/-}$ mice (9 months old) were used to isolate ubiquitinated STEP using TUBE. (**e**) NRG1β treatment results in decreased $STEP_{61}$ level and increased Tyr phosphorylation of GluN2B and ERK1/2 in cultures. Rat cortical neurons (14 days *in vitro*) were pretreated with vehicle (Veh, 0.1% dimethyl sulfoxide) or pan-ErbB receptor antagonist (PD158780, 10 μM) for 30 min, followed by NRG1β (10 nM) for 30 min. Neuronal lysates were analyzed for $STEP_{61}$, $pSTEP_{61}$ and tyrosine phosphorylation of STEP substrates. (**f**) NRG1β treatment leads to increased surface *N*-methyl D-aspartate glutamate receptors in cultures. Cortical neurons were treated with NRG1β (10 nM) for 30 min. Cells were incubated with 1.5 mg ml^{-1} Sulfo-NHS-SS-Biotin for 20 min at 4 °C, lysed in 1 × RIPA buffer. Equal amount of lysates (300 μg) was incubated with NeutrAvidin agarose to isolate biotinylated proteins, including surface receptors. Total lysates were used to measure total protein levels. (**g**) NRG1β administration normalizes $STEP_{61}$ level and restored Tyr phosphorylation of GluN2B and ERK1/2 in $Nrg1^{+/-}$ mice. Male WT and $Nrg1^{+/-}$ littermates (6–9 months old) were administered Veh (saline) or NRG1β extracellular domain (50 ng kg^{-1}, intraperitoneally) daily for 5 days. Frontal cortices were collected 3 h after the last injections and P2 fractions were used for biochemical analysis. (**h**) NRG1β treatment results in decreased $STEP_{61}$ level and increased Tyr phosphorylation of GluN2B and ERK1/2 in human neurons. SZ1-FB and control neurons were treated with NRG1β (10 nM) for 6 h. $STEP_{61}$ and phosphorylation of STEP substrates were assessed on western blotting. (**i**) NRG1 signaling leads to increased ubiquitination of $STEP_{61}$ in rat cortical neurons. Cultures were pretreated with MG-132 (10 μM) for 1 h, followed by NRG1β treatment (10 nM, 30 min). All STEP species were immunoprecipitated using anti-STEP antibody and probed with anti-ubiquitin antibody. (**j**) NRG1β treatment leads to increased ubiquitination of $STEP_{61}$ in human neurons. SZ1-FB and control neurons were pretreated with MG-132 (10 μM, 1 h), followed by NRG1β treatment (10 nM, 6 h). Ubiquitinated STEP species were pulled down using TUBE and detected by anti-STEP antibody. All data are expressed as mean ± s.e.m. and statistical significance was determined using one-way analysis of variance with Bonferroni's test (*$P < 0.05$, **$P < 0.01$, $n = 6$ each group).

in order to better define the subset of patients with increased $STEP_{61}$ levels. We predict that, particularly for these individuals, $STEP_{61}$ inhibitors might be effective therapeutic agents.

Our mouse and hiPSC findings are consistent with the glutamate hypothesis of SZ (reviewed in Coyle,[49] Javitt *et al.*[50] and Lin *et al.*[49–51]); Nrg1 signaling is a critical mediator of synaptic function and plasticity in glutamatergic signaling (reviewed in Mei *et al.*[25]) and $Nrg1^{+/-}$ mice have been reported as having miniature excitatory postsynaptic currents (mEPSCs) with faster decay and a smaller NMDA/AMPA ratio than WT littermates.[52] Deletion of ErbB4, the $Nrg1^{+/-}$ receptor, results in reduced frequency and amplitude of mEPSCs.[53] Finally, given that recombinant STEP protein decreased NMDAR currents and mEPSCs,[1] while functional inhibition[1] or genetic deletion of STEP[10] enhanced mEPSCs, and that activity-dependent regulation of STEP contributes to homeostatic stabilization of both NMDAR and AMPAR excitatory synapses,[54] it is possible that perturbations in $STEP_{61}$ contribute to glutamatergic dysfunction both in mouse models of SZ and in patients. Nonetheless, this hypothesis needs to be investigated at the circuit level in mouse models and confirmed by electrophysiology in hiPSC neurons.

Because genomic analyses have not linked variants at *PTPN5* (the gene encoding the protein STEP) to SZ, we posit that increased $STEP_{61}$ activity is a downstream biochemical consequence of other perturbations, rather than a primary cause of SZ. Increased $STEP_{61}$ levels seem to derive from disruptions in the ubiquitination and degradation of $STEP_{61}$, which are regulated, at least in part, by NRG1 signaling. This is consistent with evidence that genes involved in UPS are downregulated in postmortem SZ cortical tissue[55,56] and similar to what is observed in neurodegenerative diseases.[5,7,57] Although further work will clarify whether other mechanisms also affect $STEP_{61}$ protein levels, our findings suggest that inhibition of $STEP_{61}$ activity might prove to be a promising point of therapeutic intervention for the subset of SZ patients in which $STEP_{61}$ levels are increased.

CONFLICT OF INTEREST

The authors declare no conflict of interest.

ACKNOWLEDGMENTS

We thank laboratory members for helpful discussions and critical reading of the manuscript. This work was funded by NIH grants MH091037 and MH52711 (to PJL), GM054051 (to JAE), R01MH091861 (to CP), MH078833 (to UM), a Christopher & Dana Reeve Foundation fellowship (to CSB), the Brain and Behavior Research Foundation (to KJB), NIH grants MH101454 and MH106056 (to KJB), as well as New York Stem Cell Foundation – Robertson Award (to KJB). Kristen J Brennand is a New York Stem Cell Foundation – Robertson Investigator. As per our agreement with Coriell Cell Repository, some hiPSC lines generated from the Coriell collection control and SZ1 fibroblasts will be available from Coriell. Additionally, all Coriell collection control and SZ1 hiPSCs have been deposited at the NIMH Center for Collaborative Studies of Mental Disorders at RUCDR, and all NIMH control and SZ2 hiPSCs are currently being deposited.

AUTHOR CONTRIBUTIONS

JX conducted biochemical experiments, behavioral tests and analyzed data. PK and NC conducted biochemical analyses, CO and EF conducted behavioral tests, MX and CP conducted PPI test and analyzed the data. JR contributed SZ2 fibroblasts. KJB and BJH reprogrammed the SZ1 and SZ2 hiPSC cohorts; KJB, BJH and AT conducted SZ1- and SZ2-FB hiPSC neuronal differentiations; BJH and S-MH completed *Ngn2* inductions to yield SZ2-GLU hiPSC neurons; NS and KS contributed confocal microscopy of SZ1-FB and SZ2-GLU hiPSC neurons; SG and BA designed and conducted automated feature-based analysis of SZ1-FB and SZ2-GLU neuronal images; and AP and MN conducted SZ1-FB hiPSC neuron MEA. TDB and JAE provided TC-2153. CB and UM provided CNS-specific ErbB2/4 knockout brain lysates. JX, PJL and KJB designed the experiments. JX, ACN, PJL and KJB wrote the manuscript.

REFERENCES

1 Pelkey KA, Askalan R, Paul S, Kalia LV, Nguyen TH, Pitcher GM *et al.* Tyrosine phosphatase STEP is a tonic brake on induction of long-term potentiation. *Neuron* 2002; **34**: 127–138.
2 Bult A, Zhao F, Dirkx R Jr., Sharma E, Lukacsi E, Solimena M *et al.* STEP61: a member of a family of brain-enriched PTPs is localized to the endoplasmic reticulum. *J Neurosci* 1996; **16**: 7821–7831.
3 Boulanger LM, Lombroso PJ, Raghunathan A, During MJ, Wahle P, Naegele JR. Cellular and molecular characterization of a brain-enriched protein tyrosine phosphatase. *J Neurosci* 1995; **15**: 1532–1544.
4 Paul S, Snyder GL, Yokakura H, Picciotto MR, Nairn AC, Lombroso PJ. The Dopamine/D1 receptor mediates the phosphorylation and inactivation of the protein tyrosine phosphatase STEP via a PKA-dependent pathway. *J Neurosci* 2000; **20**: 5630–5638.
5 Kurup P, Zhang Y, Venkitaramani DV, Xu J, Lombroso PJ. The role of STEP in Alzheimer's disease. *Channels* 2010; **4**: 347–350.
6 Goebel-Goody SM, Wilson-Wallis ED, Royston S, Tagliatela SM, Naegele JR, Lombroso PJ. Genetic manipulation of STEP reverses behavioral abnormalities in a fragile X syndrome mouse model. *Genes Brain Behav* 2012; **11**: 586–600.
7 Kurup P, Xu J, Videira RA, Ononenyi C, Baltazar G, Lombroso P *et al.* STEP61 is a substrate of the E3 ligase parkin and is upregulated in Parkinson's disease. *Proc Natl Acad Sci USA* 2015; **112**: 1202–1207.
8 Goebel-Goody SM, Baum M, Paspalas CD, Fernandez SM, Carty NC, Kurup P *et al.* Therapeutic implications for striatal-enriched protein tyrosine phosphatase (STEP) in neuropsychiatric disorders. *Pharmacol Rev* 2012; **64**: 65–87.
9 Karasawa T, Lombroso PJ. Disruption of striatal-enriched protein tyrosine phosphatase (STEP) function in neuropsychiatric disorders. *Neurosci Res* 2014; **89**: 10–19.
10 Zhang Y, Kurup P, Xu J, Carty N, Fernandez SM, Nygaard HB *et al.* Genetic reduction of striatal-enriched tyrosine phosphatase (STEP) reverses cognitive and cellular deficits in an Alzheimer's disease mouse model. *Proc Natl Acad Sci USA* 2010; **107**: 19014–19019.
11 Xu J, Chatterjee M, Baguley TD, Brouillette J, Kurup P, Ghosh D *et al.* Inhibitor of the tyrosine phosphatase STEP reverses cognitive deficits in a mouse model of alzheimer's disease. *PLoS Biol* 2014; **12**: e1001923.
12 Carty NC, Xu J, Kurup P, Brouillette J, Goebel-Goody SM, Austin DR *et al.* The tyrosine phosphatase STEP: implications in schizophrenia and the molecular mechanism underlying antipsychotic medications. *Transl Psychiatry* 2012; **2**: e137.
13 Stefansson H, Sigurdsson E, Steinthorsdottir V, Bjornsdottir S, Sigmundsson T, Ghosh S *et al.* Neuregulin 1 and susceptibility to schizophrenia. *Am J Hum Genet* 2002; **71**: 877–892.
14 Barros CS, Calabrese B, Chamero P, Roberts AJ, Korzus E, Lloyd K *et al.* Impaired maturation of dendritic spines without disorganization of cortical cell layers in mice lacking NRG1/ErbB signaling in the central nervous system. *Proc Natl Acad Sci USA* 2009; **106**: 4507–4512.
15 Brennand KJ, Simone A, Jou J, Gelboin-Burkhart C, Tran N, Sangar S *et al.* Modelling schizophrenia using human induced pluripotent stem cells. *Nature* 2011; **473**: 221–225.
16 Ahn K, Gotay N, Andersen TM, Anvari AA, Gochman P, Lee Y *et al.* High rate of disease-related copy number variations in childhood onset schizophrenia. *Mol Psychiatry* 2014; **19**: 568–572.
17 Brennand K, Savas JN, Kim Y, Tran N, Simone A, Hashimoto-Torii K *et al.* Phenotypic differences in hiPSC NPCs derived from patients with schizophrenia. *Mol Psychiatry* 2015; **20**: 361–368.
18 Lee IS, Carvalho CMB, Douvaras P, Ho SM, Hartley BJ, Zuccherato LW *et al.* Characterization of molecular and cellular phenotypes associated with a heterozygous CNTNAP2 deletion using patient-derived hiPSC neural cells. *NPJ Schizophr* 2015; **1**: 15019.
19 Topol A, Zhu S, Hartley BJ, English J, Hauberg ME, Tran N *et al.* Dysregulation of miRNA-9 in a subset of schizophrenia patient-derived neural progenitor cells. *Cell Rep* 2016; **15**: 1024–1036.
20 Xu J, Kurup P, Zhang Y, Goebel-Goody SM, Wu PH, Hawasli AH *et al.* Extrasynaptic NMDA receptors couple preferentially to excitotoxicity via calpain-mediated cleavage of STEP. *J Neurosci* 2009; **29**: 9330–9343.
21 Venkitaramani DV, Paul S, Zhang Y, Kurup P, Ding L, Tressler L *et al.* Knockout of striatal enriched protein tyrosine phosphatase in mice results in increased ERK1/2 phosphorylation. *Synapse* 2009; **63**: 69–81.
22 Yang JZ, Si TM, Ruan Y, Ling YS, Han YH, Wang XL *et al.* Association study of neuregulin 1 gene with schizophrenia. *Mol Psychiatry* 2003; **8**: 706–709.
23 Munafo MR, Thiselton DL, Clark TG, Flint J. Association of the NRG1 gene and schizophrenia: a meta-analysis. *Mol Psychiatry* 2006; **11**: 539–546.
24 Del Pino I, Garcia-Frigola C, Dehorter N, Brotons-Mas JR, Alvarez-Salvado E, Martinez de Lagran M *et al.* Erbb4 deletion from fast-spiking interneurons causes schizophrenia-like phenotypes. *Neuron* 2013; **79**: 1152–1168.

25 Mei L, Xiong WC. Neuregulin 1 in neural development, synaptic plasticity and schizophrenia. *Nat Rev Neurosci* 2008; **9**: 437–452.
26 Yin DM, Chen YJ, Lu YS, Bean JC, Sathyamurthy A, Shen C *et al.* Reversal of behavioral deficits and synaptic dysfunction in mice overexpressing neuregulin 1. *Neuron* 2013; **78**: 644–657.
27 O'Tuathaigh CM, Babovic D, O'Sullivan GJ, Clifford JJ, Tighe O, Croke DT *et al.* Phenotypic characterization of spatial cognition and social behavior in mice with 'knockout' of the schizophrenia risk gene neuregulin 1. *Neuroscience* 2007; **147**: 18–27.
28 Karl T, Duffy L, Scimone A, Harvey RP, Schofield PR. Altered motor activity, exploration and anxiety in heterozygous neuregulin 1 mutant mice: implications for understanding schizophrenia. *Genes Brain Behav* 2007; **6**: 677–687.
29 Yu DX, Di Giorgio FP, Yao J, Marchetto MC, Brennand K, Wright R *et al.* Modeling hippocampal neurogenesis using human pluripotent stem cells. *Stem Cell Rep* 2014; **2**: 295–310.
30 Cui Z, Feng R, Jacobs S, Duan Y, Wang H, Cao X *et al.* Increased NR2A:NR2B ratio compresses long-term depression range and constrains long-term memory. *Sci Rep* 2013; **3**: 1036.
31 Topol A, Zhu S, Tran N, Simone A, Fang G, Brennand KJ., Altered WNT. Signaling in human induced pluripotent stem cell neural progenitor cells derived from four schizophrenia patients. *Biol Psychiatry* 2015; **78**: e29–e34.
32 Ho SM, Hartley BJ, Tcw J, Beaumont M, Stafford K, Slesinger PA *et al.* Rapid Ngn2-induction of excitatory neurons from hiPSC-derived neural progenitor cells. *Methods* 2016; **101**: 113–124.
33 Zhang Y, Pak C, Han Y, Ahlenius H, Zhang Z, Chanda S *et al.* Rapid single-step induction of functional neurons from human pluripotent stem cells. *Neuron* 2013; **78**: 785–798.
34 Venkitaramani DV, Moura PJ, Picciotto MR, Lombroso PJ. Striatal-enriched protein tyrosine phosphatase (STEP) knockout mice have enhanced hippocampal memory. *Eur J Neurosci* 2011; **33**: 2288–2298.
35 Bjarnadottir M, Misner DL, Haverfield-Gross S, Bruun S, Helgason VG, Stefansson H *et al.* Neuregulin1 (NRG1) signaling through Fyn modulates NMDA receptor phosphorylation: differential synaptic function in NRG1+/- knock-outs compared with wild-type mice. *J Neurosci* 2007; **27**: 4519–4529.
36 Hong LE, Wonodi I, Stine OC, Mitchell BD, Thaker GK. Evidence of missense mutations on the neuregulin 1 gene affecting function of prepulse inhibition. *Biol Psychiatry* 2008; **63**: 17–23.
37 Karl T, Burne TH, Van den Buuse M, Chesworth R. Do transmembrane domain neuregulin 1 mutant mice exhibit a reliable sensorimotor gating deficit? *Behav Brain Res* 2011; **223**: 336–341.
38 Xu J, Kurup P, Baguley TD, Foscue E, Ellman JA, Nairn AC *et al.* Inhibition of the tyrosine phosphatase STEP61 restores BDNF expression and reverses motor and cognitive deficits in phencyclidine-treated mice. *Cell Mol Life Sci* 2016; **73**: 1503–1514.
39 Olszewski RT, Janczura KJ, Ball SR, Madore JC, Lavin KM, Lee JC *et al.* NAAG peptidase inhibitors block cognitive deficit induced by MK-801 and motor activation induced by d-amphetamine in animal models of schizophrenia. *Transl Psychiatry* 2012; **2**: e145.
40 Nilsson M, Hansson S, Carlsson A, Carlsson ML. Differential effects of the N-methyl-d-aspartate receptor antagonist MK-801 on different stages of object recognition memory in mice. *Neuroscience* 2007; **149**: 123–130.
41 van der Staay FJ, Rutten K, Erb C, Blokland A. Effects of the cognition impairer MK-801 on learning and memory in mice and rats. *Behav Brain Res* 2011; **220**: 215–229.
42 Liljequist S, Ossowska K, Grabowska-Anden M, Anden NE. Effect of the NMDA receptor antagonist, MK-801, on locomotor activity and on the metabolism of dopamine in various brain areas of mice. *Eur J Pharmacol* 1991; **195**: 55–61.
43 Bardgett ME, Boeckman R, Krochmal D, Fernando H, Ahrens R, Csernansky JG. NMDA receptor blockade and hippocampal neuronal loss impair fear conditioning and position habit reversal in C57Bl/6 mice. *Brain Res Bull* 2003; **60**: 131–142.
44 Kurup P, Zhang Y, Xu J, Venkitaramani DV, Haroutunian V, Greengard P *et al.* Abeta-mediated NMDA receptor endocytosis in Alzheimer's disease involves ubiquitination of the tyrosine phosphatase STEP61. *J Neurosci* 2010; **30**: 5948–5957.
45 Kastin AJ, Akerstrom V, Pan W. Neuregulin-1-beta1 enters brain and spinal cord by receptor-mediated transport. *J Neurochem* 2004; **88**: 965–970.
46 Kato T, Abe Y, Sotoyama H, Kakita A, Kominami R, Hirokawa S *et al.* Transient exposure of neonatal mice to neuregulin-1 results in hyperdopaminergic states in adulthood: implication in neurodevelopmental hypothesis for schizophrenia. *Mol Psychiatry* 2011; **16**: 307–320.
47 Rosler TW, Depboylu C, Arias-Carrion O, Wozny W, Carlsson T, Hollerhage M *et al.* Biodistribution and brain permeability of the extracellular domain of neuregulin-1-beta1. *Neuropharmacology* 2011; **61**: 1413–1418.
48 Lanz TA, Joshi JJ, Reinhart V, Johnson K, Grantham LE 2nd, Volfson D. STEP levels are unchanged in pre-frontal cortex and associative striatum in post-mortem human brain samples from subjects with schizophrenia, bipolar disorder and major depressive disorder. *PLoS One* 2015; **10**: e0121744.
49 Coyle JT. NMDA receptor and schizophrenia: a brief history. *Schizophr Bull* 2012; **38**: 920–926.
50 Javitt DC, Schoepp D, Kalivas PW, Volkow ND, Zarate C, Merchant K *et al.* Translating glutamate: from pathophysiology to treatment. *Sci Transl Med* 2011; **3**: 102mr102.
51 Lin CH, Lane HY, Tsai GE. Glutamate signaling in the pathophysiology and therapy of schizophrenia. *Pharmacol Biochem Behav* 2012; **100**: 665–677.
52 Jiang L, Emmetsberger J, Talmage DA, Role LW. Type III neuregulin 1 is required for multiple forms of excitatory synaptic plasticity of mouse cortico-amygdala circuits. *J Neurosci* 2013; **33**: 9655–9666.
53 Ting AK, Chen Y, Wen L, Yin DM, Shen C, Tao Y *et al.* Neuregulin 1 promotes excitatory synapse development and function in GABAergic interneurons. *J Neurosci* 2011; **31**: 15–25.
54 Jang SS, Royston SE, Xu J, Cavaretta JP, Vest MO, Lee KY *et al.* Regulation of STEP61 and tyrosine-phosphorylation of NMDA and AMPA receptors during homeostatic synaptic plasticity. *Mol Brain* 2015; **8**: 55.
55 Arion D, Corradi JP, Tang S, Datta D, Boothe F, He A *et al.* Distinctive transcriptome alterations of prefrontal pyramidal neurons in schizophrenia and schizoaffective disorder. *Mol Psychiatry* 2015; **20**: 1397–1405.
56 Vawter MP, Crook JM, Hyde TM, Kleinman JE, Weinberger DR, Becker KG *et al.* Microarray analysis of gene expression in the prefrontal cortex in schizophrenia: a preliminary study. *Schizophr Res* 2002; **58**: 11–20.
57 Snyder EM, Nong Y, Almeida CG, Paul S, Moran T, Choi EY *et al.* Regulation of NMDA receptor trafficking by amyloid-beta. *Nat Neurosci* 2005; **8**: 1051–1058.

Supplementary Information accompanies the paper on the Molecular Psychiatry website (http://www.nature.com/mp)